The Characteristics of Electroencephalogram Signatures in Minimally Conscious State Patients Induced by General Anesthesia

Xing Jin, Zhenhu Liang*, Xin Wen, Yong Wang, Yang Bai, Xiaoyu Xia, Jianghong He, Jamie Sleigh, Xiaoli Li*

Abstract*—*Objective: **General anesthesia (GA) is necessary for surgery, even for patients in a minimally conscious state (MCS). The characteristics of the electroencephalogram (EEG) signatures of the MCS patients under GA are still unclear. *Methods*: The EEG during GA were recorded from 10 MCS patients undergoing spinal cord stimulation surgery. The power spectrum, phase-amplitude coupling (PAC), the diversity of connectivity, and the functional network were investigated. Long term recovery was assessed by the Coma Recovery Scale-Revised at one year after the surgery, and the characteristics of the patients with good or bad prognosis status were compared. *Results*: For the four MCS patients with good prognostic recovery, slow oscillation (0.1-1 Hz) and the alpha band (8-12 Hz) in the frontal areas increased during the maintenance of a surgical state of anesthesia (MOSSA), and "peak-max" and "trough-max" patterns emerged in frontal and parietal areas. During MOSSA, the six MCS patients with bad prognosis demonstrated: increased modulation index, reduced diversity of connectivity (from mean±SD of 0.877±0.003 to 0.776±0.003, p<0.001), reduced function connectivity significantly in theta band (from mean±SD of 1.032±0.043 to 0.589±0.036, p<0.001, in prefrontal-frontal; and from mean±SD of 0.989±0.043 to 0.684±0.036, p<0.001, in frontal-parietal) and reduced local and global efficiency of the network in delta band. *Conclusions*: A bad prognosis in MCS patients is associated with signs of impaired thalamocortical and cortico-cortical connectivity – as indicated by inability to produce inter-frequency coupling and phase synchronization. These indices may have a role in predicting the long-term recovery of MCS patients.**

***Index Terms*—minimally conscious state; general anesthesia; prognosis; phase-amplitude coupling; connectivity; brain network**

I. Introduction

STUDY into the neural basis of consciousness can support the diagnosis, prognosis, and treatment of disorders of consciousness (DoC) [1]. The assessment of consciousness state and the prediction of prognosis recovery are key issues in clinical practice for patients with DoC, and there is no gold standard of depth of anesthesia (DoA) monitoring to guarantee their safety during surgery [2].

The EEG reflects the numerous neuronal activities in macro-scale, which is a potential tool to quantify the anesthetic effects [3]. Recently, an adaptive reconfiguration index, which combined network hubs and directed functional connectivity based on the anesthetic EEG, was proposed to predict eventual recovery of consciousness in coma and DoC patients [4]. However, the details of the EEG changes for DoC patients were not given, thus the prediction of possible recovery of consciousness during anesthesia for the DoC patients is still needed to be investigated. The EEG spectrum is an important index for determining the DoA [5]. In adult patients without brain injury, the propofol induces a typical frontal alpha oscillation (8-12 Hz) and slow oscillation (SO) (0.1-1 Hz) at the dose levels sufficient to induced loss of consciousness (LOC)[6]; for sevoflurane, it also characterized by large alpha band power, and elicited higher power across the theta (4–8 Hz) and beta (12–25 Hz) frequency ranges [7]. However, for DoC patients, whose brain function is impaired by ischemia and hypoxia, cerebral hemorrhage and trauma [8], so the spectral patterns induced by anesthetic drugs are not still known.

The PAC plays an important role in high-level cognitive activities [9], which is an important mechanism for neuronal communication and functional connection [10]. For unconsciousness maintained by the propofol, there is a distinct frontal PAC pattern between SO and alpha in normal adults [11], which originates from the change of the thalamic-cortical circuits. It is unknown whether a distinct PAC pattern still occurs for MCS patients.

The phase-lag index between the prefrontal–frontal channel

This work was supported in part by the Scientific and Technological Innovation 2030 (STI2030-Major Projects+2021ZD0204300), the National Natural Science Foundation of China (grant numbers 62073280, 61827811), the Natural Science Fund for Distinguished Young Scholars of Hebei Province of China (F2021203033) and the Hebei Province Science and Technology Support Plan (21372001D). *(Corresponding authors: Zhenhu Liang; Xiaoli Li.)*

Xing Jin is with the School of Artificial Intelligence, Xidian University, Xi'an, China

Zhenhu Liang is with the Institute of Electrical Engineering, Yanshan University, Qinhuangdao, China (e-mail: zhl@ysu.edu.cn)

Xin Wen is with the Institute of Electrical Engineering, Yanshan University, Qinhuangdao, China

Yong Wang is with the Key Laboratory of Intelligent Rehabilitation and Neuromodulation of Hebei Province, Qinhuangdao, China

Yang Bai is with the Department of Basic Medical Science, School of Medicine, Hangzhou Normal University, Hangzhou, Zhejiang, China

Xiaoyu Xia is with the Senior Department of Neurosurgery, the First Medical Center of PLA General Hospital, Beijing, China

Jianghong He is with the Department of Neurosurgery, Beijing Tiantan Hospital, Capital Medical University, Beijing, China

Jamie Sleigh is with the Department of Anesthesia, Waikato Clinical School, University of Auckland, Hamilton, New Zealand

Xiaoli Li is with the State Key Laboratory of Cognitive Neuroscience and Learning & IDG/McGovern Institute for Brain Research, Beijing, Normal University, Beijing, China (e-mail: xiaoli@bnu.edu.cn)

pairs significantly decreases for the duration of anesthesia [12]. Recently, a new measure named phase-lag entropy (PLE) was proposed to measure the diversity of the phase synchronization between two signals, and may be a better index of the level of consciousness during general anesthesia [12]. This diversity of connectivity patterns induced by general anesthesia could be an important index for assessing the level of consciousness for patents with MCS as well.

The corticocortical connectivity has been considered as a key discriminator between conscious and unconscious states in human [13, 14], and frontal-parietal connectivity can be used to reflect anesthetic unconsciousness due to a variety of anesthetics [13-15]. The dynamical fluctuations in connection are significant during anesthesia in the alpha and theta bands [16, 17]. However, it is unclear whether this connectivity and the global and local network can be used to predict the prognosis of patients with MCS.

This study aims to: (1) explore the EEG characteristics induced by general anesthesia for patients with MCS; (2) demonstrate the EEG characteristics induced by general anesthesia could predict the prognosis of recovery of consciousness for MCS patients.

II. Materials and Methods

A. Participants and EEG recordings

We recorded the EEG from ten MCS patients (*N*=10, 6 male, 4 female, age=42.80 ± 10.62 yr., weight=59.00 ± 10.22 kg) undergoing a SCS implant surgery at the PLA General Hospital, Beijing, China. The patients met the following inclusion criteria: (1) patients had been diagnosed as MCS by the Coma recovery scale-revised (CRS-R); (2) patients were in a stable clinical condition; and (3) there were no confounding complications (e.g., infections). The patients' legal representatives signed the informed consent form before surgery. The protocol was approved by the PLA Army General Hospital ethics committee (No: 2017-33). All patients had remained stable for at least 1.5 months (10.25±8.52). The details of the patients' information are presented in Supplement Table S1.

A 32-channel EEG cap (BrainAmp 64 MRplus, Brain Products, Germany) with Ag/AgCl electrodes was adopted for EEG recording. The positions of the electrodes were set according to the international 10/20 system. Conductive EEG gel was applied to remove cutin and oil from subjects' scalps. The electrode–skin impedance of subjects was decreased to less than 5 kΩ before the recording. The EEGs were recorded from resting state to MOSSA and recovery state, with the sampling rate of 1 kHz. Since there is currently no gold standard for determining a MCS patient's loss of consciousness, the experienced anesthesiologists termed the time of fixed eyeball and no eyelash reflection as the time point as LOC, and the dosages of the anesthetics were performed according to the standard dosing requirements (i.e., the same as for patients without MCS). The induction drugs were sufentanil (0.2-0.6μg/kg), rocuronium bromide (0.2-1mg/kg), and propofol (1-2mg/kg), and maintenance drug was propofol (3.6-4.3mg/kg/h) (*N*=4) or sevoflurane (the concentration of 2~4%) (*N*=6). The two types of anesthesia were propofol-propofol (induced by propofol and maintained by propofol) and propofol-sevoflurane (induced by propofol and maintained by sevoflurane), respectively. The entire recording process lasted approximately 60 minutes for each MCS patient (among it, the MCS-resting state lasts about 10 minutes, the induction period 10 minutes, the MOSSA 25 minutes, and the MCS-recovery state 15 minutes). This is an approximate time, depending on the situation, and not all patients have the same recorded time. After surgery, the consciousness state of the patients were confirmed by CRS-R, heart rate and blood oxygen. Each MCS patient undergoes three times CSR-R assessments while awake, each taking approximately 1 hour. And the highest score was taken as the patient's CSR-R score. We contacted the patients for the recovery information after one year. We divided the patients who died or not show any improvement of CRS-R score into bad group (2 propofol-propofol and 4 propofol-sevoflurane), and who had behaviors related to consciousness and improvement of CRS-R scores into good group (2 propofol-propofol and 2 propofol-sevoflurane).

B. EEG preprocessing

The EEG data were preprocessed for off-line analysis by using EEGLAB toolbox (version 12.0.2.5b) in MATLAB environment (version 2020a). Firstly, large-amplitude EEG artifacts were removed and the bad channels were rejected by visual inspection. Secondly, an adaptive notch filter was utilized to remove the 50 Hz power frequency artifact. Then, a band-pass filter was used to extract the EEG data from 0.1 Hz to 40 Hz, and the EEG signal was resampled to 100 Hz by running *resample.m* in MATLAB. Finally, relevant components of the artifacts, such as electromyography and eye movements, were identified and removed by independent component analysis (ICA) [18, 19], which is based on EEGLAB toolbox and performed for per MCS patients. ICA components resemble EMG activity (high-frequency power relative to low-frequency power, highly localized scalp origin, i.e. high spatial kurtosis and EMG-like temporal structure, i.e. spiking activity) and EOG-like activity (temporal sparse and intense activation, prefrontal topography and symmetric or asymmetric polarity, corresponding to blinks or eye movements). Artifactual components were removed (5.42±1.76), and the residual components were back-projected to the electrode space. In order to unify the data length convenient analysis, we select 2-minute electroencephalogram segments during MCS-resting state, 3-minute segments during MOSSA and 2-minute segments during MCS-recovery state from all subjects. The EEG data in the MCS-resting state, MOSSA and MCS-recovery state at the frontal, parietal and occipital regions were analyzed in details. Because the EEG signatures of frontal, parietal, and occipital regions are highly related with the change of consciousness, we only analyzed the EEG features of these regions. As seen in Fig. S1A, seven EEG channels in each region (Frontal: Fp1, Fp2, F3, F4, F7, F8, and Fz; Parietal: CP1, CP2, P3, P4, P7, P8 and Pz; Occipital: PO3, PO4, PO7, PO8, O1, O2, and Oz) were enrolled for extraction of the indices. The raw EEG signal of six channels (two frontal

channels (Fp1 and Fp2), two parietal channels (P3 and P4) and two occipital channels (O1 and O2)) and the amplified 5 second waveform of Fp1 were shown in Fig. S1B. It can be seen that the amplitude of the EEG increased and the waveform trended towards low frequencies after induction.

C. Power spectrum analysis

We computed the spectrograms of the EEG during the general anesthesia process using the multitaper method as implemented in the Chronux toolbox (version 2.11; http://chronux.org/. Accessed July 15, 2018) with window lengths of T= 2 s with 1 s overlap, time-bandwidth product TW=3, number of tapers K=5. In this study, we analyzed the frequency bands of SO (0.1-1 Hz), delta (1-4 Hz), theta (4-8 Hz), alpha (8-13 Hz), beta (13-30 Hz), and gamma (30-40 Hz). The group-level spectrogram was obtained by averaging the spectrograms from all available channels and concatenating the three states previously described.

D. Phase-amplitude coupling analysis

PAC refers to a neural mechanism in which the phase of an oscillation at a lower frequency modulates the occurrence of activity at a higher frequency. To quantity the strength of PAC, modulation index (MI) based on the Kullback-Leibler divergence was utilized [20]. The time-varying phase-amplitude modulogram was employed to characterize the PAC pattern of specific frequency bands in resting state, MOSSA, and recovery. The detailed computation of PAC is presented in Supplement Part I. The MI reflects the strength of phase-amplitude coupling, it ranges from 0 to 1.

E. Phase lag entropy analysis

PLE is a measure of the diversity of connections between the two phase series, which incorporates the temporal dynamics of the instantaneous phase series into the phase synchronization analysis [12, 21, 22]. The algorithm for calculating PLE is presented in Supplement Part II. If there is a stereotypic interaction over time between two EEG series at the different areas, there is a dominant phase pattern, then the PLE would be low. It was notes that the PLE is a measure of the diversity of connectivity patterns, not the connection strength of the two series.

F. Network analysis

The functional connectivity was estimated using weighted phase lag index (wPLI)[23], which is a phase synchronous measurement method that is relatively resistant to volume conduction and reference montage effects by considering only non-zero phase lead/lag relationships [23]. Given two signals $x(t)$ and $y(t)$, the wPLI is defined as[17]

$$wPLI = \left| \frac{\sum_{t=1}^{n} \left| imag\left(S_{xy,t}\right) \right| \operatorname{sgn}\left(imag\left(S_{xy,t}\right)\right)}{\sum_{t=1}^{n} \left| imag\left(S_{xy,t}\right) \right|} \right| \quad (1)$$

where S_{xy} is the complex cross-spectral density of two real-valued signals $x(t)$ and $y(t)$. The wPLI is based only on the virtual component of the cross spectrum and is therefore robust to noise compared to coherence because unrelated noise sources cause an increase in signal power [1].

For implementation, wPLI was computed using the *Fieldtrip toolbox*. The EEG signals were divided into 30-s windows with a 90% overlap, which was further divided into 2-s sub-windows with a 50% overlap. For each sub-window, the cross-spectral density was estimated using the multitaper method, with time-bandwidth product=3 and the number of tapers=5; from these repetitions the wPLI values were estimated as a function of frequency. In this study, we studied on the frontal-parietal connectivity as the averaged wPLI index across the combinations between channels of F3, F4, Fz, F7, F8 and P3, P4, Pz, P7, P8, CP1, CP2, and prefrontal-frontal connectivity as the averaged wPLI index between channels of Fp1, Fp2, and F3, F4, Fz, F7, F8, for these regions are implicated in anesthetic-induced unconsciousness [16, 17].

In the present study, we analyzed the both local and global network metrics. The local characteristics of the brain network were measured by the nodal clustering coefficient (CC) and the nodal efficiency (NE). Global characteristics of the brain network were measured by normalized clustering coefficient (NCC) and normalized path length (NPL). The EEG electrodes were regarded as the nodes in graph, and the wPLI values between two electrodes were considered as the edges in graph. The detailed computations of the network parameters are presented in Supplement Part III.

G. Statistical analysis

This study evaluated the changes of EEG characteristics in MCS patients during general anesthesia. Because of the exploratory nature of the study, no a priori statistical power calculation was conducted to guide sample size. We calculated the MI of every coupling style, the wPLI, the nodal clustering coefficients and the nodal efficiency. To evaluate these features, we used the Lilliefors test (*lillietest.m*) to determine whether the sample fits into a normally distributed population, then we applied generalized linear mixed models (GLMM) using Satterthwaite's method to analyze the interaction effects of the two factors: state (MCS-resting, MOSSA, MCS-recovery); and prognosis status (good prognosis and bad prognosis). The fixed effects are the state and the prognosis, and the random effect is the random intercept of each subject. After obtaining the interaction effects and the main effects of the two factors, a *post hoc* comparisons were done using the Tukey's test. The mean and 95% confidence interval (CI) values of the estimated difference were reported. The effect size for the mixed effects model was calculated by Cohen's *d*, which is an effect size measure to express the difference between two means relative to their standard deviation. If the value of adjusted *p* is less than 0.05, the statistical result is considered significant [24, 25], and $p<0.05$, $p<0.01$, $p<0.001$ were marked with "*", "**", and "***" in figures, respectively.

III. Results

A. The EEG spectral characteristics of MCS patients during general anesthesia

The EEG spectrogram is an important signature to investigate the effect of anesthetic drugs during general anesthesia. Because we maintained anesthesia with two different anesthetic drugs, i.e. propofol and sevoflurane, we analyzed the EEG power spectra of these two drugs, respectively. We calculated the averaged spectrogram and power spectra of frontal, parietal and occipital areas, respectively. Fig. 1A showed the averaged EEG spectrogram and power spectra of a good prognosis patient during propofol-propofol anesthesia. It can be seen that the power of SO in MOSSA is higher and the power of high frequency (beta and gamma) is lower than MCS-resting and MCS-recovery in frontal, parietal and occipital regions. There is an increase of power in alpha band only in the frontal region during MOSSA, and this change is similar to normal patients. These changes were absent in the bad prognosis patients (Fig. S2A). An example of a good prognosis patient from the propofol-sevoflurane group is shown in Fig. 1B. The power in low frequencies (<4Hz) increased in frontal and parietal channels, but, again, was absent in bad prognosis patients (Fig. S2B).

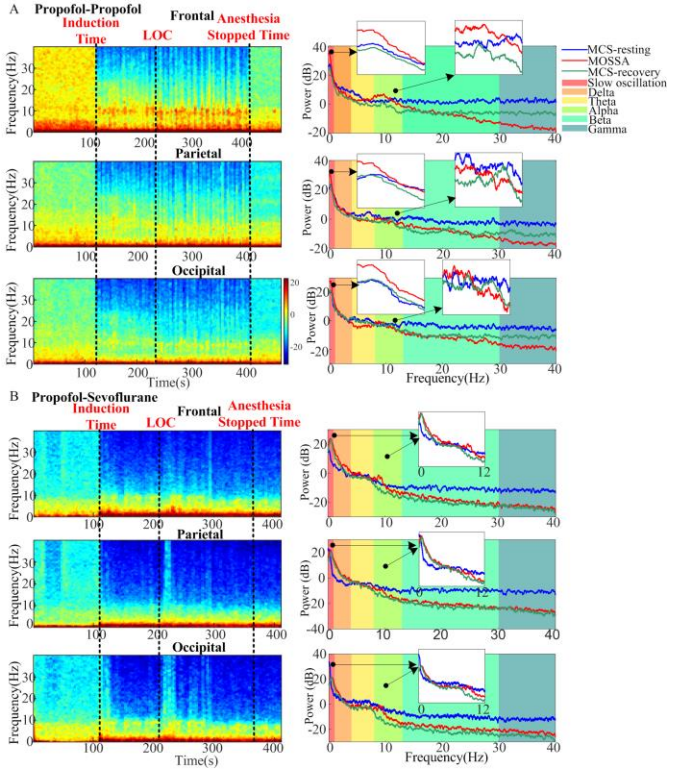

Fig. 1. The averaged spectrogram and power spectral in frontal, parietal and temporal throughout the whole propofol-propofol (**A**) and propofol-sevoflurane (**B**) general anesthesia of the good prognosis patient, respectively. For each patient, the power spectrogram was averaged over frontal, parietal and occipital channels. The white box in (**A**) show the amplification of the corresponding frequency band (left: SO; right: alpha). And show the frequency 0.1-12Hz in (**B**).

B. State-converting phase-amplitude modulation during general anesthesia

We calculated the PAC of the MCS patients. The phase of low frequency (0.1-8 Hz) with steps of 1 Hz and amplitude of high frequency (1-40 Hz) with steps of 2 Hz were set for calculation. The group averaged co-modulograms of all channels in frontal, parietal and occipital region of a good prognosis patient during propofol-propofol anesthesia were shown in Fig. 2A. Obviously, there was an increased coupling strength between the phase of 0.1-1 Hz oscillations and amplitude of 1-40 Hz oscillations in the MOSSA state. Fig. 2B presented the group averaged phase-ampograms between 0.1-1 Hz and 1-40 Hz for the different states. In MOSSA state, we can see a distinct "peak-max" pattern in frontal regions and a "trough-max" pattern in parietal regions, but no distinct pattern in occipital regions. Fig. 2C showed the averaged phase shifts in different brain regions, which presents a different changes of frontal and parietal channels in the MOSSA state. In frontal, the high frequency band amplitude was either evenly spread over SO phase in MCS-resting and MCS-recovery, and was greater near the peak of the SO in MOSSA, resulting in a "peak-max" distribution. But in parietal, the distribution shifted towards "trough-max" with greater high frequency amplitude near SO troughs in MOSSA. The spatial representation of the co-modulograms and the phaseampograms of the patient were shown in Fig.S3A and Fig.S4A, respectively. Fig. 2D shows the averaged co-modulograms of a good prognosis patient from the propofol-sevoflurane anesthesia. It can be seen that the coupling strength increased between the phase of 0.1-1 Hz oscillations and amplitude of 1-40 Hz oscillations in the MOSSA state. In Fig. 2E and Fig. 2F, we can also see a "peak-max" pattern in frontal channels and a "trough-max" pattern in parietal channels, but in occipital channels, there emerged a "fall-max" pattern (the definition of this pattern was described in our previous study[26]), the high frequency band amplitude was greater near the falling edge of the SO phase in MOSSA. The spatial distribution of the co-modulograms and the phaseampograms of the same patient were shown in Fig.S3B and Fig.S4B, respectively.

The changes of PAC patterns of SO-alpha have been proved to be an important biomarker in propofol-induced loss of consciousness and recovery of consciousness [27]. To assess the relationship between PAC pattern and prognosis, we demonstrate the SO-alpha PAC pattern of a good and a bad prognosis patient respectively (Fig. S5A and Fig. S5B) during the anesthesia process. The results show that only the good prognosis patient has distinct PAC patterns between SO and alpha; as per healthy patients [28-30]. A distinct "peak-max" pattern emerged in frontal area and a "trough-max" pattern in most parietal and occipital areas after induction. The percentages of patients with good prognosis that showed both "peak-max" and "trough-max" patterns, which were significantly higher in frontal (84%), parietal (83.3%) and occipital (75%) areas than that of patients with a bad prognosis (47.6%, 45.2% and 35.7%, respectively), the results are in Supplement Table S2.

We further analyzed the MI of nine different frequency modulation pairs (SO-alpha, SO-beta, SO-gamma, delta-alpha, delta-beta, delta-gamma, theta-alpha, theta-beta, and theta-gamma). We analyzed the patients with good and bad prognosis

separately. The boxplots of MI values between the two different groups (i.e., propofol-propofol and propofol-sevoflurane) during MOSSA were shown in Fig.S6. There is no significant difference in all paired frequency bands, so we combined the two drug groups for statistical analysis of MI, shown in Fig. 3. The statistics results showed that the MI can significantly differentiate the good and bad prognosis in MOSSA in all the modulation pairs ($p<0.05$, Tukey's test) except SO-gamma and delta-gamma. Moreover, the MI in SO-alpha, SO-beta, SO-gamma, delta-gamma frequency bands of the good and bad prognosis patients among in MOSSA are all significantly higher than those from MCS-resting and MCS-recovery periods($p<0.001$, Tukey's test). The detailed statistics were presented in Supplement Table S3 (theta-alpha, theta-beta, and theta-gamma were excluded for analysis because the values are too small).

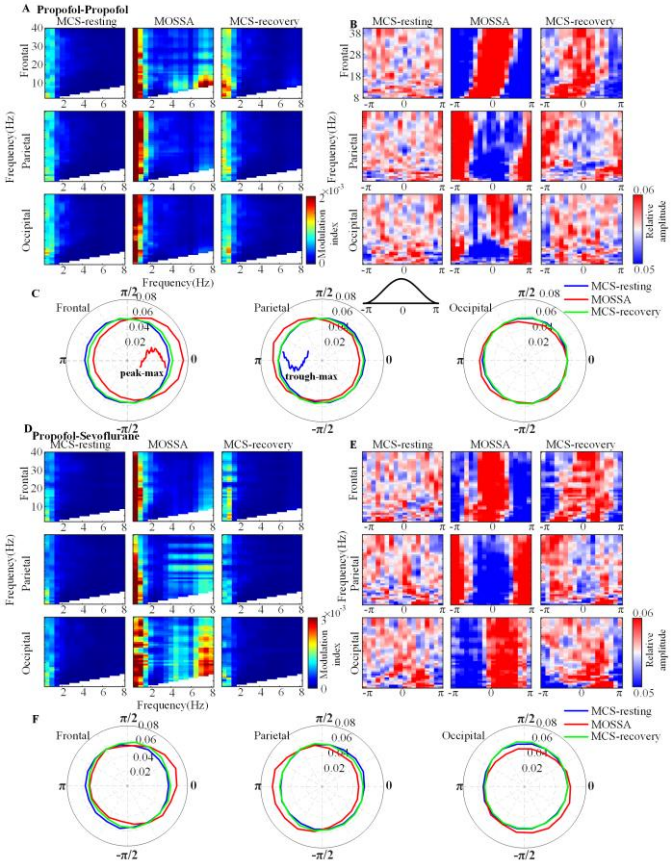

Fig. 2. The averaged co-modulograms of low frequency band (0.1-8 Hz, step is 1Hz) and high frequency band (1-40 Hz, step is 2 Hz) (**A**) (**D**); the phaseampograms between SO and high frequency band (**B**) (**E**); and the averaged phase shifts (**C**) (**F**) of all channels in frontal, parietal and occipital region of the good prognosis patient during propofol-propofol and propofol-sevoflurane anesthesia, respectively. (**C**) and (**F**) using angular histograms of the high frequency band amplitude distributed over SO phase.

C. The phase lag entropy decreased during MOSSA in MCS patients

We analyzed the synchronization changes of EEG channels within and between regions during GA. The boxplots of PLE values of two drugs during MOSSA are presented in Fig. S7A and showed no significant difference, so we combined the two drug groups for a statistical analysis of PLE as regards prognosis. For a good prognosis patient, Fig. 4A showed the changes of mean PLE of all paired-EEG channels among F-P (frontal-parietal), F-O (frontal-occipital) and P-O (parietal-occipital). The details of PLE between all channels in three regions are shown in Fig. 4B. It decreased during MOSSA and then increased in the MCS-recovery state. To get a clearer view of how the brain regions are connected with each other, we chose the top 30 percent of the PLE connections (there are 210 kinds of connections, the figure only showed the top 63 kinds) in every state (Fig. 5C).

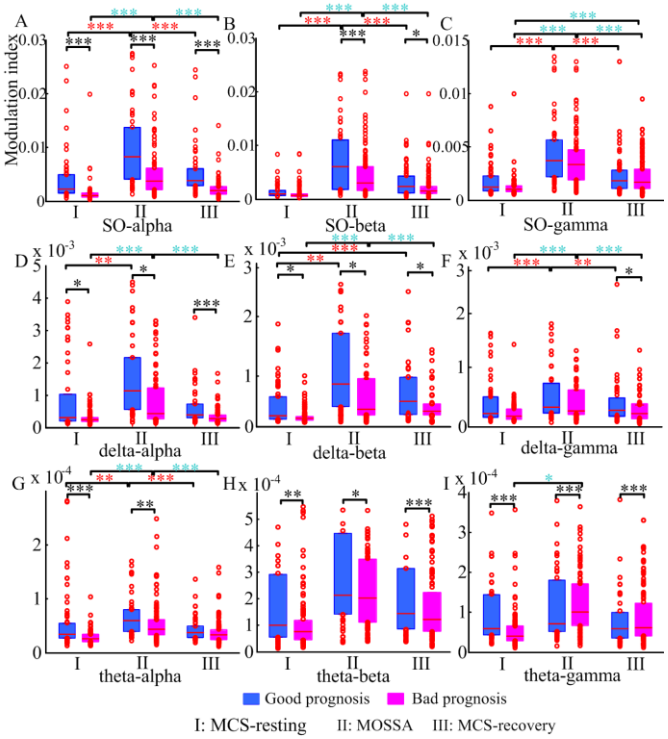

Fig. 3. The statistical of modulation index of different coupling styles in MCS-resting, MOSSA and MCS-recovery of both good and bad prognosis patients. (**A**)-(**I**) represent the statistical results of SO-alpha, delta-alpha, theta-alpha, SO-beta, delta-beta, theta-beta, SO-gamma, delta-gamma and theta-gamma coupling styles, respectively. And the MI were averaged from the windows of different anesthesia states.

The boxplots of both good and bad prognosis patients were shown in Fig. 4D. The result of Fig. 4B and Fig. 4C presented no obviously different among channels, so we put all channel pairs together for statistical analysis. The *post hoc* comparison showed that the PLE of both good and bad prognosis can distinguish the anesthesia states ($p<0.001$). Also, the PLE of the bad prognosis patients for MCS-resting, MOSSA and MCS-recovery states are all significantly higher than good prognosis patients ($p<0.001$) (the results of significance were shown in Supplement Table S4). The mean and SD values of the PLE indices are given in Supplement Table S5.

D. Dynamic connectivity during anesthesia induced changes of MCS patients

The individual-level connectivity data from the perioperative period of a good prognosis patient is presented in Fig.S8, the connectivity had obvious changes in delta, theta and alpha bands in the different states for prefrontal-frontal and frontal-parietal connectivity. But for a bad prognosis patient (Fig. S9),

there was no significant changes in any frequency bands and states. So, we discuss the connectivity statistics in three bands (delta, theta, alpha). Fig. 5A, Fig. 5C and Fig. 5E show the averaged wPLI of three states in delta band, theta band and alpha band, respectively. The statistical results of three bands for good and bad prognosis are shown in Fig. 5B, Fig. 5D and Fig. 5F. The averaged wPLI for the theta and alpha bands, in particular, showed significant changes in MOSSA ($p<0.001$ and $p=0.037$) for the good prognosis patients. Compared to the bad prognosis group, the wPLI index of good prognosis patients in MOSSA of theta in prefrontal-frontal and frontal–parietal connectivity was significantly higher (0.78 ± 0.57 to 0.59 ± 0.48, $p<0.001$; 0.81 ± 0.54 to 0.68 ± 0.54, $p=0.021$). There was no significant difference between prefrontal–frontal and frontal–parietal for every state. The mean and SD values of the wPLI indices in different postoperative states and bands shown in Supplement Table S6.

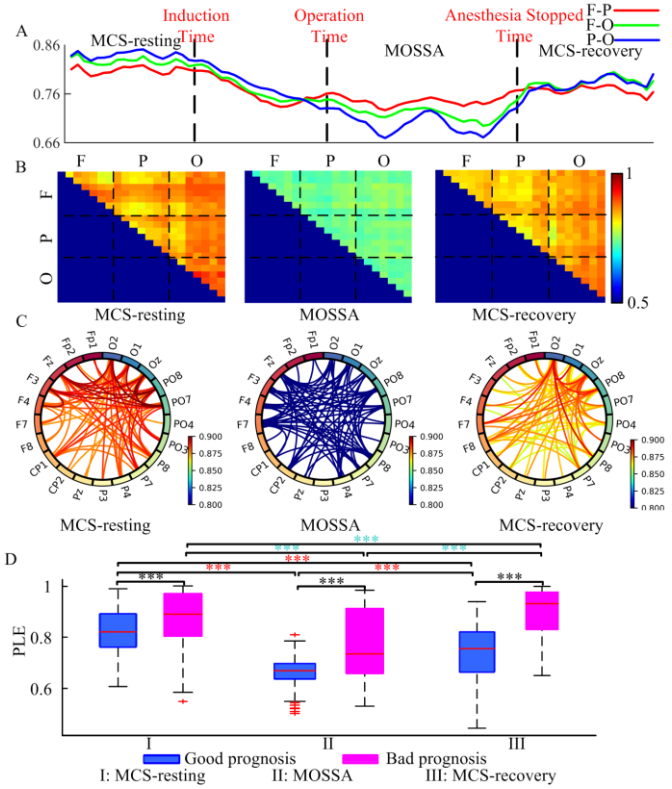

Fig. 4. The result of the averaged phase-lag entropy (PLE) analysis. (**A**) The mean PLE of all MCS patients among F-P (frontal-parietal), F-O (frontal-occipital) and P-O (parietal-occipital). (**B**) The details of averaged PLE between channels in all three regions. (**C**) The top 30 percent of the PLE connection (there are 210 kinds of connections, the figure only showed the top 63 kinds) in every state of good prognosis patients. (**D**) And the PLE statistic were averaged from the windows of states of MCS-resting, MOSSA and MCS-recovery for all MCS patients.

E. The changes of network at nodal and global levels during anesthesia

To investigate the nodal and global changes of functional connectivity at delta, theta and alpha frequencies during anesthesia, we performed graph theory-based network analysis and contrasted different graph measures between good and bad prognosis groups. We constructed the networks based on the wPLI, which was regarded as the edge in graph theory. Since there were no significant differences between propofol-propofol group and propofol-sevoflurane group for the wPLI index (Fig. S7B), we statistically analyzed the brain networks for both groups together. The network metrics of CC and NE of one good prognosis patient at delta frequency band are shown in Fig. 6A and Fig. 6C, respectively. The curves for the mean of CC and NE are presented in Fig. 6B and Fig. 6D. The statistical analysis showed that the CC and NE values were significantly increased in MOSSA ($p<0.001$, Tukey's test), and then decreased in MCS-recovery, showed in Fig. 6E and Fig. 6F. The CC and the NE of good prognosis patients is higher than the bad prognosis patients in MOSSA ($p<0.01$) and MCS-recovery ($p<0.001$), and is lower in MCS-resting. Detailed statistical results were shown in Supplement Table S7. The CC and NE in theta band (Fig. S10) showed the same trends as delta band in anesthesia procedure, but in MOSSA, the two indices of good prognosis patients was lower than that of bad prognosis patients ($p<0.001$). However, there was no significant change in alpha band (Fig. S11) among states and between different prognosis groups.

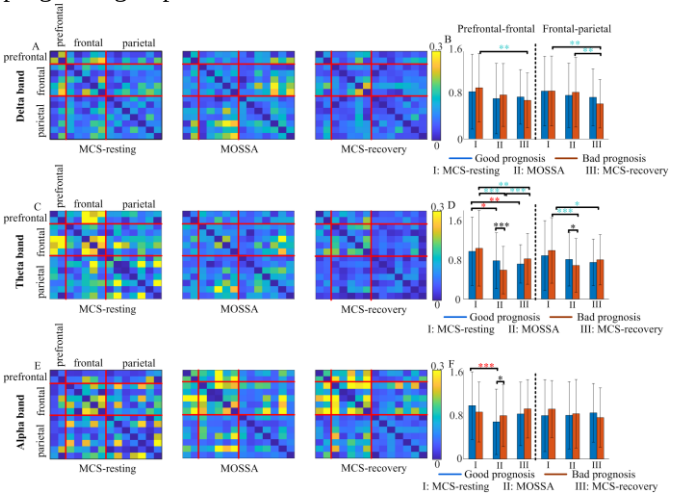

Fig. 5. (**A**) (**C**) (**E**) The colour maps of averaged individual wPLI between different areas in delta, theta and alpha bands, respectively. (**B**) (**D**) (**F**) The mean and SD of wPLI values at alpha, theta, and delta bands in all good and bad prognosis patients. The wPLI statistic were averaged from the windows of states of MCS-resting, MOSSA and MCS-recovery for all MCS patients.

To investigate the global network changes, we analyzed the normalized average clustering coefficient (C_{nor}), normalized average path length (L_{nor}), and small worldness (σ). Fig. 6G revealed the evolution of C_{nor} and L_{nor} for one good prognosis patient. Fig. 6H, Fig. 6I and Fig. 6J showed the statistics of delta band for C_{nor}, L_{nor} and the σ property of all MCS patients. No significant difference was shown between MCS-resting and MOSSA states in these indices. In MOSSA, the C_{nor} and σ of bad prognosis are significantly higher ($p<0.01$ and $p<0.001$) than good prognosis group. The results of theta and alpha bands are shown in Fig. S12 and Fig. S13. The mean and SD of MCS-resting, MOSSA and MCS-recovery were shown in Supplement Table S8.

The above results indicate that the brain network of a bad prognosis patient is closer to a completely random network; and

the global brain network structures were not affected much by anesthetic, because the MCS patients are more or less in a state of global dysfunction. Especially, the average small worldness property of all states for both prognosis groups are less than 1, which indicates that the MCS patients didn't have a small worldness property (σ >1).

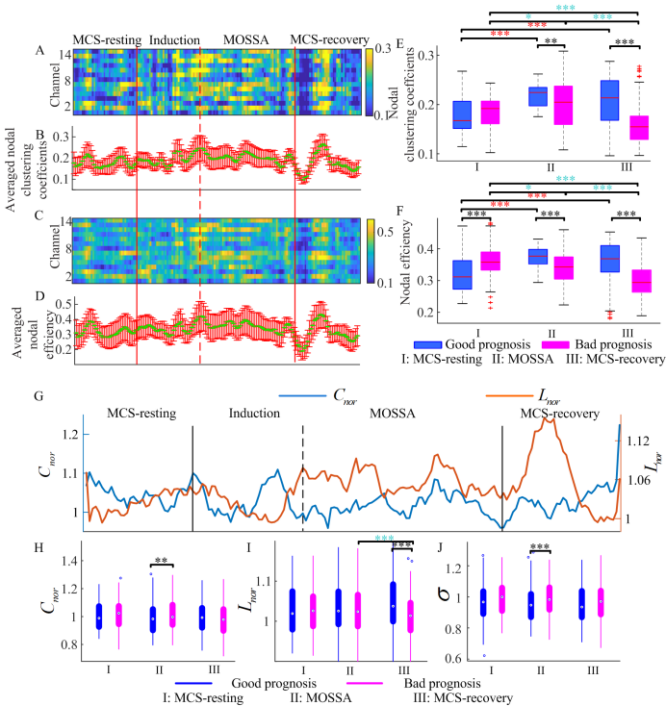

Fig. 6. The time course of network parameters at delta band. (**A**) Nodal clustering coefficient for the whole anesthesia procedure. (**B**) The curve for the mean and standard deviation (SD) for nodal clustering coefficient. (**C**) Nodal efficiency for the whole anesthesia procedure. (**D**) The curve for the mean and standard deviation (SD) for nodal efficiency. (**A-D**) is of the good prognosis patients (**E**) Boxplots of nodal clustering coefficient and (**F**) nodal efficiency for both good and bad prognosis patients. (**G**) The C_{nor} (blue curve) and L_{nor} (orange curve) of one good prognosis MCS patient for MCS-resting, MOSSA and MCS-recovery at delta band. (**H**)-(**J**) The statistics of the C_{nor} , L_{nor} and σ for all patients in MCS-resting, MOSSA and MCS-recovery.

IV. Discussion

Consciousness is a multifaceted concept with two main components [31, 32]: (1) awareness of environment and self (i.e. the content of consciousness); (2) wakefulness (i.e. the level of consciousness). Based on this framework, the level and content of consciousness both decrease during GA for normal patients. However, for the MCS patients, their brain is maintained with low or no content of consciousness (awareness) but with a certain level of consciousness (wakefulness). So, the process of anesthetic induced unconsciousness for the MCS patients provides a unique way to investigate the consciousness. Further, a recent study [4] proposed that the propofol induced brain network reconfiguration provided a new way to predict the consciousness recovery of coma and DoC patients. We hypothesized that the EEG characteristics during the GA could also predict the consciousness recovery for MCS patients.

In this study, we analyzed the EEG features of MCS patients during propofol-propofol and propofol-sevoflurane GA. The EEG spectrogram and power spectral, cross frequency coupling (i.e., PAC), the diversity of connectivity patterns (i.e., PLE), the function connectivity (i.e., wPLI) and brain network metrics at nodal and global level were studied. Our study provides an important way for investigating the mechanism of anesthetic-drug effects in MCS patients, and supplies the underlying EEG biomarkers for depth of anesthesia monitoring and consciousness recovery prognostication.

A. EEG spectral features during general anesthesia can predict the prognosis

In this study, we systematically analyzed the EEG spectrogram and power spectra of MCS patients during propofol-propofol and propofol-sevoflurane general anesthesia. In the propofol-propofol group, we found the power of SO and alpha increased in MOSSA only in good prognosis patients. In the propofol-sevoflurane group the low frequency (<4Hz) power increased in good prognosis patients only. Previous studies have found a distinct SO and alpha oscillation peak emerged in propofol induced GA in normal patients [29, 33]. Phenomenologically, the alpha rhythm emerged in the frontal area while it is appeared in the occipital area [29]. However, all these phenomena didn't appear in MCS patients who had bad prognosis. Because the MCS patients may have undergone pathway damage of the thalamocortical system, we hypothesized the damaged pathway influences a normal projection of depolarization and hyperpolarization between thalamus and cortex. Therefore, the EEG power and spectrum are important features for analyzing the prognosis in MCS patients.

B. Phase amplitude coupling may be a potentially important prognostic indicator

We analyzed the PAC strength (i.e., MI) and PAC pattern in MCS patients in this study. Various studies have shown that cross-frequency coupling plays an important role in high level cognitive activities in the brain for mental health patients [20, 28, 34]. But this method is rarely used in MCS patients, and there is no benchmark to measure the coupling between the phase of low frequency bands and the amplitude of high frequency bands in MCS patients. Thus, we calculated the MI for a wide range of frequency bands. From the results we found that MI increased significantly in most coupling pairs in the MOSSA state for both good and poor prognosis patients but not drug (propofol-propofol and propofol-sevofluane) related. In normal patients, the MI in SO-alpha, SO-beta increases in propofol-induced GA [28, 35] Alcauter et al. also found that cortical-thalamic and thalamocortical connections are highly correlated with EEG oscillations in SO-delta and alpha [36]. This proves that the anesthetics influence thalamic-cortical connection (highly related with the level of consciousness) and MI can also measure the change in MCS patients. Also, in SO-alpha, SO-beta, delta-alpha and delta-beta bands, we found that the good prognosis group was significantly higher than the bad prognosis group ($p<0.001$) in MOSSA. As we know, thalamic injury is an important cause of consciousness impairment in DoC patients [37]. Combined with the differences of good

prognosis and bad prognosis in PAC, we suggested that MI is a potential predictive EEG biomarker for the prognosis of MCS patients.

Previous studies have found two distinct PAC patterns, "peak-max" and "trough-max", between SO and alpha during propofol-induced GA in normal humans [28, 29]. Therefore, the pattern change of PAC has become an important mark for LOC. We also found the two patterns in MCS patients, and these frontal "peak-max" patterns and parietal "trough-max" patterns only emerged in the patients who went on to have a good prognosis. This indicates that the PAC pattern reflects the integrity or robustness of brain function, and can be as a prognostic biomarker.

C. The phase lag entropy can distinguish the anesthesia states and predict the prognosis in MCS patients

Disruption of cortico-cortical connectivity has been suggested to be a central role in explaining the GA, sleep and DoC associated unconsciousness [38]. In this study, we used the PLE to measure the cortico-cortical connectivity patterns between different channels in same or different regions. It was found to be useful as a hypnotic depth indicator in patients receiving propofol sedation [21, 22], and can effectively qualify the cortico-cortical communication during general anesthesia [39]. In our study, the PLE index decreased significantly in MOSSA in both good and bad prognosis patients, which was similar to that of normal patients, and indicates that anesthesia induced a decrease in phase-lag pattern diversity and an increase in phase synchronization.

Also, the PLE values of the bad prognosis group were higher ($p<0.001$) than the good prognosis group in three states, which illustrated the PLE have the ability to predict the recovery of patients' consciousness. Laureys et al. found in rare cases where patients in a vegetative state recover awareness, the PET showed a functional recovery of metabolism in the same cortical regions [37]. We speculate our result may be related with the relatively intact and unimpaired brain functional connection over a cortical scale in good prognosis patients.

D. The changes of connectivity and network throughout the general anesthesia

The study assessed the cortical connectivity throughout the GA of patients with MCS. Results showed different patterns of dynamic cortical connectivity throughout the perioperative period. The wPLI didn't have the strong ability to distinguish between different anesthesia states of MCS. Propofol disrupts the cortical integration both, within- and between-network connectivity [40]. We observed an increase in global and local efficiency in the delta band and theta band during the transition to MOSSA. Some studies have shown that the patients with consciousness disorders have higher local efficiency than in healthy controls in delta and theta bands [1], they also highlighted a higher level of structural connectivity in patients' theta band with the same topological measurements compared to healthy controls. At lower frequencies, patients' networks are denser, more interconnected and even more similar than those in healthy brains. This funding is consistent with our results. As with fMRI networks in coma reported by Achard et al. [41], the modular structure of alpha band networks in DoC patients were neither consistently similar to healthy controls, nor to each other. We found no significant change in alpha band neither in local nor global efficiency, which confirmed the conclusion of Achard et al.. This suggests that there may be some degree of reorganization of brain networks in DoC, rather than just disorganization. Also, we found that the CC and NE in the delta band can differentiate the good from bad prognosis groups in all three states; and in the theta band can differentiate the good from bad prognosis in MOSSA. For bad prognosis patients, the synchronization and connection between brain regions was disrupted at a certain degree and the brain networks are more disordered and random, which indicate that the self-organizing capability of the brain is compromised more seriously [42]. This suggested that a lack of processes which regulate functional interactions between brain regions may be responsible for patients' inability to regain consciousness.

There are several limitations in our study. First, the sample size was relatively small, and our findings are preliminary and need to be validated in a larger cohort of patients with different behavioral and demographic characteristics and with different types of brain and chronic injuries. Second, the drugs used to maintain general anesthesia were inconsistent. We statistically analyzed separate groups for some indicators, and we made a unified analysis for the indicators showed no difference between the two drugs. Third, our current analysis lacked a control group experiment, so we need to supplement the data for further analysis in the future. At the same time, doing an age matching and drug matching research can be of great significance. Finally, we only performed statistical analysis on whether each index can distinguish between anesthesia status and prognosis, so our next research will further enhance our conclusions through feature selection and classification, and discusses how each indicator and its combination are valuable for the prognosis of MCS patients.

V. Conclusion

This study analyzed the EEG features of MCS patients during GA, and found that the PAC pattern, MI, PLE, the local and global efficiency in delta and beta bands all have the ability for brain state monitoring. The changes of PAC pattern, MI and PLE during GA have the potential to predict the long term prognosis for recovery of consciousness in patients with disorder of consciousness. Patients who ended up with a good recovery had better thalamo-cortical (PAC) and cortico-cortical (PLE) communication before treatment than patients with a bad prognosis. Our findings shed light on monitoring anesthesia state and predicting postoperative recovery of patients in minimally conscious state.

Appendix

Supplementary data to this article can be found online.

Acknowledgment

The authors thank the PLA Army General Hospital for

supplying the EEG data of MCS patients.

REFERENCES

[1] S. Chennu et al., "Spectral signatures of reorganised brain networks in disorders of consciousness," *PLoS Comput Biol,* vol. 10, no. 10, pp. e1003887, Oct, 2014.

[2] T. Yamamoto et al., "Spinal cord stimulation for treatment of patients in the minimally conscious state," *Neurol Med Chir (Tokyo),* vol. 52, no. 7, pp. 475-81, 2012.

[3] A. E. Soplata et al., "Thalamocortical control of propofol phase-amplitude coupling," *PLoS Comput Biol,* vol. 13, no. 12, pp. e1005879, Dec, 2017.

[4] C. Duclos et al., "Brain Responses to Propofol in Advance of Recovery From Coma and Disorders of Consciousness: A Preliminary Study," *Am J Respir Crit Care Med*, Nov, 2021.

[5] P. L. Purdon et al., "Clinical Electroencephalography for Anesthesiologists: Part I: Background and Basic Signatures," *Anesthesiology,* vol. 123, no. 4, pp. 937-60, Oct, 2015.

[6] C. E. Warnaby et al., "Investigation of Slow-wave Activity Saturation during Surgical Anesthesia Reveals a Signature of Neural Inertia in Humans," *Anesthesiology,* vol. 127, no. 4, pp. 645-657, Oct, 2017.

[7] O. Akeju et al., "Effects of sevoflurane and propofol on frontal electroencephalogram power and coherence," *Anesthesiology,* vol. 121, no. 5, pp. 990-8, Nov, 2014.

[8] J. L. Bernat, "Chronic disorders of consciousness," *Lancet,* vol. 367, no. 9517, pp. 1181-92, Apr, 2006.

[9] D. Li et al., "Cross-frequency coupling during isoflurane anaesthesia as revealed by electroencephalographic harmonic wavelet bicoherence," *Br J Anaesth,* vol. 110, no. 3, pp. 409-19, Mar, 2013.

[10] R. T. Canolty, and R. T. Knight, "The functional role of cross-frequency coupling," *Trends Cogn Sci,* vol. 14, no. 11, pp. 506-15, Nov, 2010.

[11] J. M. Lee et al., "A Prospective Study of Age-dependent Changes in Propofol-induced Electroencephalogram Oscillations in Children," *Anesthesiology,* vol. 127, no. 2, pp. 293-306, Aug, 2017.

[12] H. Lee et al., "Diversity of functional connectivity patterns is reduced in propofol-induced unconsciousness," *Hum Brain Mapp,* vol. 38, no. 10, pp. 4980-4995, Oct, 2017.

[13] M. Boly et al., "Connectivity changes underlying spectral EEG changes during propofol-induced loss of consciousness," *J Neurosci,* vol. 32, no. 20, pp. 7082-90, May, 2012.

[14] J. Schrouff et al., "Brain functional integration decreases during propofol-induced loss of consciousness," *Neuroimage,* vol. 57, no. 1, pp. 198-205, Jul, 2011.

[15] D. Jordan et al., "Simultaneous electroencephalographic and functional magnetic resonance imaging indicate impaired cortical top-down processing in association with anesthetic-induced unconsciousness," *Anesthesiology,* vol. 119, no. 5, pp. 1031-42, Nov, 2013.

[16] P. E. Vlisides et al., "Dynamic Cortical Connectivity during General Anesthesia in Surgical Patients," *Anesthesiology,* vol. 130, no. 6, pp. 885-897, Jun, 2019.

[17] D. Li et al., "Dynamic Cortical Connectivity during General Anesthesia in Healthy Volunteers," *Anesthesiology,* vol. 130, no. 6, pp. 870-884, Jun, 2019.

[18] Z. Liang et al., "Information Integration and Mesoscopic Cortical Connectivity during Propofol Anesthesia," *Anesthesiology,* vol. 132, no. 3, pp. 504-24, Nov, 2020.

[19] D. Whitmer et al., "Utility of independent component analysis for interpretation of intracranial EEG," *Front Hum Neurosci,* vol. 4, pp. 184, 2010.

[20] R. Zhang et al., "Temporal-spatial characteristics of phase-amplitude coupling in electrocorticogram for human temporal lobe epilepsy," *Clin Neurophysiol,* vol. 128, no. 9, pp. 1707-1718, Sep, 2017.

[21] H. W. Shin et al., "Monitoring of anesthetic depth and EEG band power using phase lag entropy during propofol anesthesia," *BMC Anesthesiol,* vol. 20, no. 1, pp. 49, Feb, 2020.

[22] S. Ki et al., "Phase lag entropy as a hypnotic depth indicator during propofol sedation," *Anaesthesia,* vol. 74, no. 8, pp. 1033-1040, Aug, 2019.

[23] M. Vinck et al., "An improved index of phase-synchronization for electrophysiological data in the presence of volume-conduction, noise and sample-size bias," *Neuroimage,* vol. 55, no. 4, pp. 1548-65, Apr, 2011.

[24] P. Xie et al., "Direct Interaction on Specific Frequency Bands in Functional Corticomuscular Coupling," *IEEE Trans Biomed Eng,* vol. 67, no. 3, pp. 762-772, Mar, 2020.

[25] X. Wang et al., "Neuromodulation Effects of Ultrasound Stimulation Under Different Parameters on Mouse Motor Cortex," *IEEE Trans Biomed Eng,* vol. 67, no. 1, pp. 291-297, Jan, 2020.

[26] Z. Liang et al., "Propofol Anesthesia Decreased the Efficiency of Long-Range Cortical Interaction in Humans," *IEEE Trans Biomed Eng,* vol. 69, no. 1, pp. 165-175, Jan, 2022.

[27] A. Scheinin et al., "Differentiating Drug-related and State-related Effects of Dexmedetomidine and Propofol on the Electroencephalogram," *Anesthesiology,* vol. 129, no. 1, pp. 22-36, Jul, 2018.

[28] E. A. Mukamel et al., "A transition in brain state during propofol-induced unconsciousness," *J Neurosci,* vol. 34, no. 3, pp. 839-45, Jan, 2014.

[29] P. L. Purdon et al., "Electroencephalogram signatures of loss and recovery of consciousness from propofol," *Proc Natl Acad Sci U S A,* vol. 110, no. 12, pp. E1142-51, Mar, 2013.

[30] E. A. Mukamel et al., "Phase-based measures of cross-frequency coupling in brain electrical dynamics under general anesthesia," *Annu Int Conf IEEE Eng Med Biol Soc,* vol. 2011, pp. 1981-4, 2011.

[31] S. Laureys, "The neural correlate of (un)awareness: lessons from the vegetative state," *Trends Cogn Sci,* vol. 9, no. 12, pp. 556-9, Dec, 2005.

[32] Z. Liang et al., "Constructing a Consciousness Meter Based on the Combination of Non-Linear Measurements and Genetic Algorithm-Based Support Vector Machine," *IEEE Trans Neural Syst Rehabil Eng,* vol. 28, no. 2, pp. 399-408, Feb, 2020.

[33] Z. Liang et al., "Age-dependent cross frequency coupling features from children to adults during general anesthesia," *Neuroimage,* vol. 240, pp. 118372, Oct, 2021.

[34] B. Lega et al., "Slow-Theta-to-Gamma Phase-Amplitude Coupling in Human Hippocampus Supports the Formation of New Episodic Memories," *Cereb Cortex,* vol. 26, no. 1, pp. 268-278, Jan, 2016.

[35] L. Ma et al., "Propofol Anesthesia Increases Long-range Frontoparietal Corticocortical Interaction in the Oculomotor Circuit in Macaque Monkeys," *Anesthesiology,* vol. 130, no. 4, pp. 560-571, Apr, 2019.

[36] S. Alcauter et al., "Development of thalamocortical connectivity during infancy and its cognitive correlations," *J Neurosci,* vol. 34, no. 27, pp. 9067-75, Jul 2014.

[37] S. Laureys et al., "Brain function in coma, vegetative state, and related disorders," *Lancet Neurol,* vol. 3, no. 9, pp. 537-46, Sep, 2004.

[38] O. Akeju et al., "Disruption of thalamic functional connectivity is a neural correlate of dexmedetomidine-induced unconsciousness," *Elife,* vol. 3, pp. e04499, Nov 2014.

[39] M. R. Jun et al., "Assessment of phase-lag entropy, a new measure of electroencephalographic signals, for propofol-induced sedation," *Korean J Anesthesiol,* vol. 72, no. 4, pp. 351-356, Aug, 2019.

[40] L. D. Lewis et al., "Rapid fragmentation of neuronal networks at the onset of propofol-induced unconsciousness," *Proc Natl Acad Sci U S A,* vol. 109, no. 49, pp. E3377-86, Dec, 2012.

[41] M. M. Monti et al., "Dynamic change of global and local information processing in propofol-induced loss and recovery of consciousness," *PLoS Comput Biol,* vol. 9, no. 10, pp. e1003271, 2013.

[42] S. Laureys et al., "Impaired effective cortical connectivity in vegetative state: preliminary investigation using PET," *Neuroimage,* vol. 9, no. 4, pp. 377-82, Apr, 1999.